Sentinel pipe racks quantify orthophosphate's effect on lead release into drinking water

Benjamin F. Trueman[§,*], Wendy H. Krkošek[†], and Graham A. Gagnon[§]

[§]Centre for Water Resources Studies, Department of Civil & Resource Engineering, Dalhousie University, 1360 Barrington St., Halifax, Nova Scotia, Canada B3H 4R2

[†]Halifax Water, 450 Cowie Hill Rd., Halifax, Nova Scotia, Canada, B3P 2V3

*Corresponding author
E-mail: benjamin.trueman@dal.ca
Tel:902.494.6070
Fax: 902.494.3105

Abstract

Orthophosphate is used widely to control lead release from plumbing into tap water. Its effect can be difficult to quantify, though, since tap water lead concentrations are site-specific. Sentinel homes with lead service lines are ideal for evaluating orthophosphate corrosion control programs, but best practices dictate the removal of lead service lines once they are identified. Sentinel homes, then, often have too short a useful life to be used effectively. Here we explore an alternative: sentinel pipe racks constructed with recovered lead pipes and supplied with water directly from the distribution system. We also propose a strategy for analyzing pipe rack data based on the generalized additive model, which approximates time series as a sum of smooth functions. In this study, geometric mean lead release from pipe racks exhibited a pronounced dose response, falling by 54% (95% credible interval: 14–77%) after an increase from 1 to 2 mg PO_4 L^{-1}, and then climbing by 55% (95% credible interval: 5–143%) after a decrease to 1.5 mg PO_4 L^{-1}. Data from the sentinel homes were largely consistent with those from pipe racks: geometric mean lead levels at the high orthophosphate dose (2 mg L^{-1}) were 60% of those at the low dose (1 mg L^{-1}, 95% credible interval: 50–76%). Our results demonstrate sentinel pipe racks as a viable alternative to at-the-tap sampling for non-

regulatory corrosion control monitoring. They also provide a fully Bayesian framework for quantifying orthophosphate's effect on lead release that is well-suited to incorporating information from multiple sources.

Keywords: EPA LCRR; Health Canada; corrosion control; generalized additive model; Bayesian multilevel model

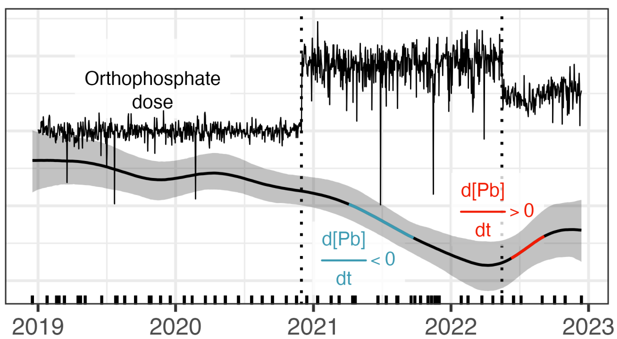

Introduction

Updated regulations on lead in drinking water promise to expedite replacement of lead service lines in Canada and the USA. Even afterwards, though, a substantial legacy of lead plumbing—including lead:tin solder and brass—will have to be managed. This will require careful control of drinking water chemistry to limit lead solubility and maintain durable corrosion scale.

Orthophosphate is an important tool to that end.[1–4] It works by forming low-solubility lead-phosphate minerals like pyromorphite ($Pb_5(PO_4)_3(Cl,F,OH)$)[5] and phosphohedyphane ($Ca_2Pb_3(PO_4)_3(Cl,F,OH)$.[6] Sometimes, it can be effective without forming a lead-phosphate phase,[7] perhaps by blocking active sites on lead carbonate surfaces[8,9] or by forming an amorphous diffusion barrier with iron, aluminum, manganese, or calcium.[10,11]

It can be difficult, though, to estimate orthophosphate's effect on lead in drinking water since lead concentrations are determined by site-specific plumbing characteristics. And while lead solubility modeling can be informative, it fails to account for the complex mineralogy of lead corrosion scale or the generation of particles.[11,12] A decrease in tap water lead sampled at sentinel homes over time is the most reliable metric of orthophosphate's success, and homes supplied by lead service lines represent the population most at-risk.[13] But to protect the inhabitants' health, lead pipe is often replaced once identified. Sentinel homes, then, may have too short a life to be useful in monitoring plumbosolvency changes.

Here we describe an alternative: sentinel lead pipe racks operated with feedwater directly from the distribution system. While they overlap in form and function with pipe loops and bench apparatus, sentinel pipe racks are designed to estimate lead release from representative lead pipes into distributed drinking water with as much precision and accuracy as possible—in as close to real-time as possible. Sentinel pipe racks can be used to understand the effect of an unplanned change in water quality, whereas pipe loop and bench-top studies are usually designed with a specific research question in mind. And while no simple model can fully replicate the complexities of premises plumbing,[14] pipe rack systems are probably a better approximation than benchtop apparatus.[15]

We present data from three separate racks, located at three sites within the Halifax Regional Municipality, a medium-sized Canadian city. We used a robust hierarchical Bayesian generalized additive model with continuous-time autoregressive errors[16] to estimate the effect on lead release of a dose increase from 1 to 2 mg PO_4 L^{-1}. Then, we used this estimate as a prior probability for the same effect in nine sentinel homes. Finally, we quantified the orthophosphate dose response of a subset of the pipe racks at 1, 2, and then 1.5 mg PO_4 L^{-1}. Our results provide a fully Bayesian framework for analyzing corrosion control treatment data, especially when they are collected as time series and have multiple sources.

Materials and methods

Data were collected in a single water system with two zones supplied by different source waters and treatment plants. Zone 1 is supplied by a conventional treatment plant employing alum coagulation, flocculation, clarification, and filtration. Zone 2 is supplied by a plant employing alum coagulation, flocculation, and direct filtration. Across the two zones, thousands of lead service lines remain, all of which will be replaced by 2038 as a part of the utility's comprehensive replacement program.[17]

Water quality

Water quality from both sources is well suited to orthophosphate corrosion control treatment,[18,19] with a pooled median pH and dissolved inorganic carbon concentration in pipe rack effluent of 7.3 and 4.4 mg C L^{-1} (Table 1). And while water quality in Zones 1 and 2 was largely similar, aluminum concentrations were markedly different: aluminum in Zone 2 was seasonal, with peak concentrations occurring at the coldest water temperatures.[20] Aluminum concentrations in Zone 1 were much lower and more consistent throughout the year (Table S1).

Table 1. Summary of water quality in pipe rack effluent; these pooled estimates represent both zones (zone-specific water quality is summarized in Table S1).

Parameter	Unit	Median	Lower quartile	Upper quartile
Dissolved Chloride	mg L^{-1}	8.4	7.9	9.4
Dissolved Inorganic Carbon	mg C L^{-1}	4.4	4.1	4.9
Free Chlorine	mg L^{-1}	0.7	0.2	0.8
Total Organic Carbon	mg C L^{-1}	1.8	1.7	2.0
pH		7.3	7.2	7.4
Turbidity	NTU	0.1	0.1	0.2

Data collection

Sentinel pipe racks

Pipe racks were installed in utility-owned infrastructure; two were located in Zone 1 and one in Zone 2. Each was fitted with four replicate recovered lead pipe sections, supplied in parallel with water from the distribution system (an example is shown in Figure S1). Each pipe was excavated and handled according to principles outlined in a recent paper[21] and was approximately 60 cm long with an internal diameter of 1.3 cm. Each was connected to plastic tubing at either end with a brass compression fitting, yielding two galvanic lead-brass connections per pipe. A timed valve supplied flow to the pipe sections for two minutes every six hours, and samples were collected approximately monthly, as the valves opened, at a nominal flow rate of 8 L min^{-1}.

Sentinel homes

Of the nine sentinel homes, seven were supplied by partial lead service lines (private lead, public copper) and the remaining two by copper service lines; all were located in Zone 2. At each sampling round, volunteer residents collected four consecutive 1L samples, starting with the first-draw after a minimum six-hour stagnation period. This 4 $\times$ 1L profile was followed first by a 10-minute flush of the plumbing and then by collection of a final 1L sample. Sample profiles were collected in May–June 2021, at 1 mg PO_4 L^{-1}, and again in May–June 2022, at 2 mg PO_4 L^{-1}. An example instruction sheet provided to residents is included as Figure S2. During the study, all residents were provided with pitcher filters certified by NSF for removal of lead.

Analytical methods

An accredited laboratory measured lead, iron, manganese, zinc, and aluminum,[22] as well as dissolved inorganic and total organic carbon,[23] chloride,[24] sulfate,[25] orthophosphate,[26] and alkalinity[27] in pipe rack effluent samples. Turbidity, pH, free chlorine, temperature, conductivity, dissolved oxygen, and oxygen reduction potential were determined onsite using portable Hach instruments. Orthophosphate was also quantified[26] in treated water by Zone 1 and 2 treatment plant staff.

Data analysis

We used R,[28] and a collection of contributed packages,[29–43] to analyze and visualize the data. The code and data necessary to reproduce the main results of the paper are available online.[44]

Sentinel pipe racks

Lead in pipe rack effluent, y_t, was modeled using a robust hierarchical Bayesian generalized additive model (GAM) with continuous-time first-order autoregressive errors.[16,45–47] The model is specified in equation (1),

$$
\begin{aligned}
&\text{likelihood:}\\
&log(y_t) \sim T(\mu_t, \sigma, \nu)\\
&\text{model for } \mu_t\text{:}\\
&\mu_t = \alpha_{pipe_i} + \sum_{j=1}^{n} f_j\,(t) + \phi^s r_{t-s}\\
&f_j(t) = X_j \beta_j + Z_j b_j\\
&r_{t-s} = log(y_{t-s}) - \alpha_{pipe_i} - \sum_{j=1}^{n} f_j\,(t-s)\\
&\text{priors:}\\
&\sigma \sim Half\text{-}T(0,2.5,3)\\
&\nu \sim Gamma(2,0.1)\\
&\phi \sim N(0.5,0.25)\\
&\alpha_{pipe_i} \sim N(\bar{\alpha}, \sigma_\alpha)\\
&\bar{\alpha} \sim T(4.2,2.5,3)\\
&\sigma_\alpha \sim Half\text{-}T(0,2.5,3)\\
&\beta_j \sim T(0,2.5,3)\\
&b_j \sim N(0, \sigma_b)\\
&\sigma_b \sim Half\text{-}T(0,2.5,3)
\end{aligned}
\qquad (1)
$$

where T denotes the Student t-distribution with time-varying mean μ_t, standard deviation σ, and degrees-of-freedom parameter ν. The mean is modeled as the sum of smooth functions of time $f_j(t)$. The full model (Zones 1 and 2) included a pipe-specific intercept α_{pipe_i} and centered smooth terms, whereas the Zone 1 model included noncentered series-specific smooths and a global intercept ($\bar{\alpha}$ in place of α_{pipe_i} in equation (1)). The matrices Z_j and X_j represent the penalized and unpenalized basis functions comprising each of the $f_j(t)$, and b_j and β_j represent the penalized and unpenalized GAM coefficients. $Gamma$ and N denote the gamma and normal distributions.

On the log scale, the time-varying mean in the full model was estimated as the sum of a global multi-year trend, a set of local multi-year trends modifying the global trend to better fit the data from each location, and a second set of local multi-year trends capturing deviations of the individual time series from the global and location-level trends (Figure S3a). Since orthophosphate was increased on different dates in Zones 1 and 2, we expressed time as days before and after the respective increases. The time-varying mean in the Zone 1 model was estimated as the sum of a global multi-year trend, a seasonal trend, and a set of local multi-year trends capturing deviations of the individual time series from the global and seasonal trends (Figure S4). In both models, the multi-year trends were estimated using thin-plate regression splines, and the Zone 1 model's seasonal trend was estimated using a cyclic cubic regression spline.[43]

The instantaneous rate of change in mean log lead concentration was estimated using finite differences, as described in a recent paper.[16] Briefly, we generated posterior predictions of the global or location-level multi-year trend along a regular time sequence spanning the range of the data. Then, we repeated this process after adding a small δ to each value in the sequence. The difference between posterior predictions evaluated at t and $t + \delta$, divided by δ, approximates the first derivative of the smooth term.

Sentinel homes

Lead concentrations in point-of-use samples, y_i, were described using a multilevel model.[48] That is, the change in lead release accompanying the orthophosphate dose increase was estimated after accounting for the effects of sample location and profile litre. The model is specified in equation (2),

$$
\begin{aligned}
&\text{likelihood:}\\
&log(y_i)|censored = 0 \sim T(\mu_i, \sigma)\\
&log(y_i)|censored = 1 \sim T\text{-}CDF(\mu_i, \sigma)\\
\\
&\text{model for } \mu_i\text{:}\\
&\mu_i = \alpha_{site_j} + \gamma_{sample_k} + \beta R\\
\\
&\text{priors:}\\
&\sigma \sim Half\text{-}N(0,1)\\
&\nu \sim Gamma(2,0.1)\\
&\beta \sim N(-0.8,0.3)\\
\\
&\alpha_{site_j} \sim N(\bar{\alpha}, \sigma_\alpha), \text{ for } j \text{ in } 1..9\\
&\bar{\alpha} \sim N(0,1)\\
&\sigma_\alpha \sim Half\text{-}Cauchy(0,1)\\
\\
&\gamma_{sample_k} \sim N\left(0, \sigma_\gamma\right), \text{ for } k \text{ in } 1..45\\
&\sigma_\gamma \sim Half\text{-}Cauchy(0,1)
\end{aligned}
\tag{2}
$$

where T again denotes the Student t-distribution with mean μ, standard deviation σ, and degrees-of-freedom ν; $censored$ is a binary variable indicating whether the sample concentration was observed or left-censored (i.e., a nondetect). The parameters α_{site_j} and γ_{sample_k} are random intercepts describing each unique site/profile litre combination, R is a binary variable indicating the sampling round (i.e., before/after the dose increase), and β is the difference between rounds. $Half\text{-}Cauchy$, and $T\text{-}CDF$ represent the half-Cauchy distribution and the Student t cumulative distribution function (i.e., $P(X \leq x)$). $T\text{-}CDF$ quantifies the probability that y_i is less than the censoring limit on the log scale. Nondetects, then, inform the model without the need to replace them with imputed values.

The priors on $\bar{\alpha}$, $\bar{\gamma}$, σ_α , and σ_γ are weakly informative, meaning that they discourage unrealistic parameter estimates.[49] The prior on β—the difference between lead concentration at the two orthophosphate doses—was determined using posterior predictions from the generalized additive model of pipe loop data, as described in the results section.

Results and discussion

Quantifying the effect of an orthophosphate dose increase

Sentinel pipe racks

Lead release from pipe racks was relatively constant at 1 mg PO_4 L^{-1} (Figure 1c). At this dose, a 95% credible interval on the slope of the global multi-year trend—capturing variation common to all pipe sections—included 0 μg Pb L^{-1} d^{-1} at all times (d[Pb]/dt ~ 0, Figure 1a). Pipe racks, then, appear to have been successfully stabilized at the initial orthophosphate concentration.

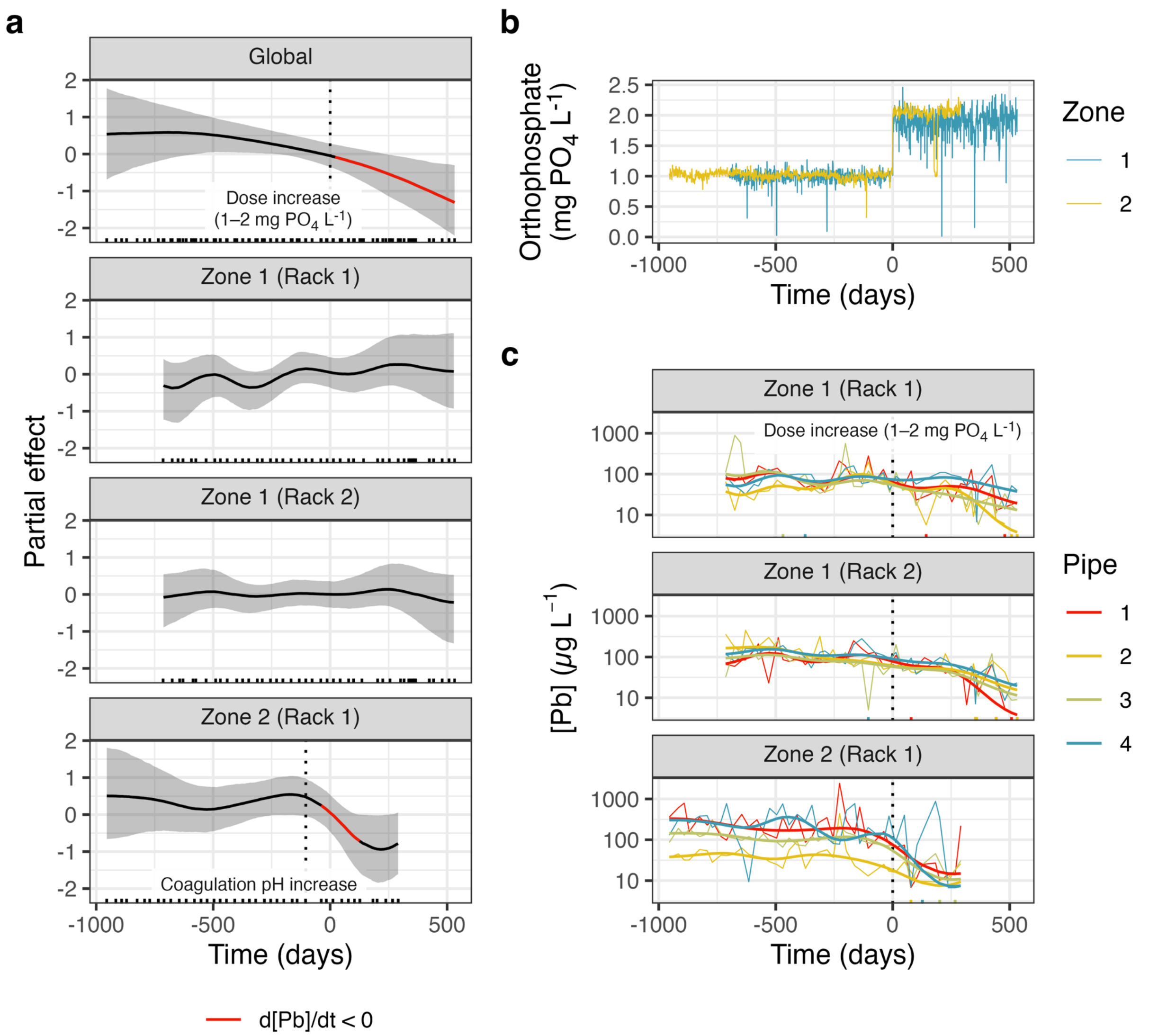

Figure 1. (a) The global multi-year smooth term representing the change in lead concentration across all pipe sections, and the local modifiers representing deviations from the global trend to better fit data from each pipe rack. Red highlighting indicates the portion of the trend where a 95% credible interval on its slope does not include zero, and the shaded grey region represents a 95% credible interval on the time-varying mean. Sample collection dates are indicated by vertical ticks on the x-axis. **(b)** Orthophosphate in treated water, by zone. **(c)** Time series of total lead in effluent from lead pipes at three locations. Fitted values from the hierarchical GAM are superimposed on the time series in bold. Ticks at the top and bottom of the panels represent values outside the plotting limits.

An increase to 2 mg PO_4 L^{-1} was followed by a decreasing trend in lead concentration (Figure 1a, c). That is, a 95% credible interval on the slope of the global multi-year trend excluded 0 μg Pb L^{-1} d^{-1} for a period beginning shortly after the dose increase and running until the end of the study period (d[Pb]/dt < 0, Figure 1a). The higher dose, then, appeared to provide additional protection against lead release. Across both zones and all three pipe racks, doubling the orthophosphate dose decreased geometric mean lead concentrations within a year by an estimated 54% (95% credible interval: 14–77%).

An additional decrease in lead release was particular to Zone 2 and not accounted for by the global trend (Figure 1a). A possible explanation was a modified treatment process: coagulation pH at the Zone 2 treatment plant was increased from less than 6 to approximately 6.3 in April 2021 (Figure S3b), to target the pH of minimum aluminum hydroxide solubility.[50] This lowered aluminum in treated water (Figure S5), and a decrease in the aluminum concentration predicts a decrease in lead solubility—assuming that some fraction of dissolved aluminum precipitates with orthophosphate, leaving less available to react with lead.[20] Less aluminum in solution may also mean less post-precipitation of aluminum as particles and less adsorption of lead to those particles. And since suspended colloids containing aluminum and lead have been identified in Zone 2,[20] the increase in coagulation pH may have decreased the capacity of distributed water to transport lead. Moreover, an improved coagulation process would be expected to remove more of the natural organic matter fractions that increase lead solubility by complexation,[51] but these fractions were not measured in treated water.

The decrease in the location-specific trend representing Zone 2 followed closely the increase in coagulation pH, and neither of the Zone 1 trends decreased comparably (Figure 1b). Furthermore, a 95% credible interval on the slope of the Zone 2 trend excluded 0 μg Pb L^{-1} d^{-1} for several months, beginning shortly after the pH increase (d[Pb]/dt < 0, Figure 1b). Changes to the coagulation process, then, appear to have lowered lead release: between the coagulation pH increase and the orthophosphate dose increase, geometric mean lead decreased by an estimated 34% (95% credible interval: 0–57%). Since only a short period separated the pH increase and the change in orthophosphate dose, controlling for orthophosphate's effect yielded a more reliable estimate of the coagulation pH effect. That is, the hierarchical nature of the model allows us to control for an effect common to all groups to better understand an effect that occurred in only one group.

Sentinel homes

We used the estimated year-over-year decrease in geometric mean lead release from pipe racks (54%) as a prior probability for orthophosphate's effect on lead concentrations in the sentinel homes' tap water (Figure 2a). The prior probability reflects our state of knowledge before learning from the point-of-use data; on the natural log scale, an approximation of the prior difference estimate is $N(\mu = -0.8, \sigma = 0.3)$, where N is a Gaussian with mean μ and standard deviation σ.

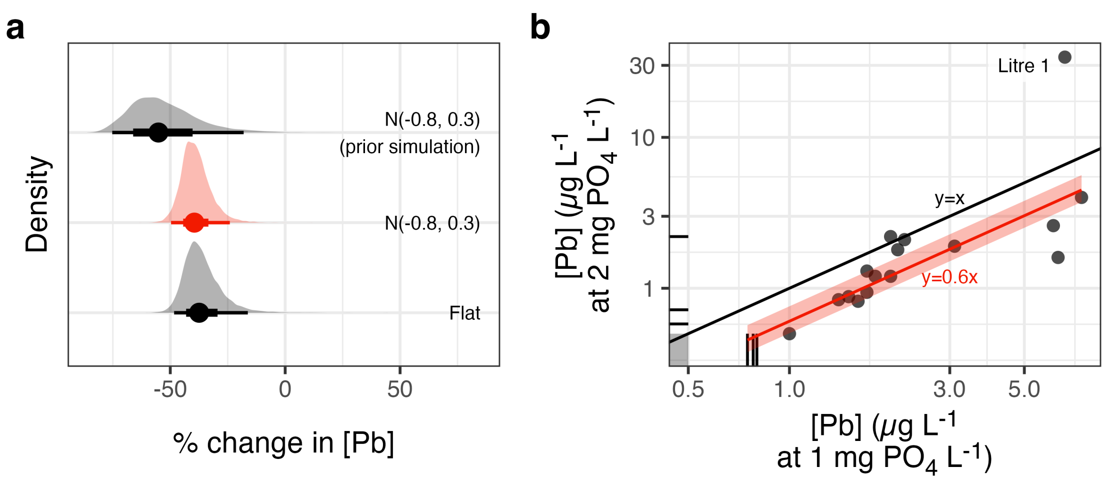

Figure 2. (a) Density plots show the estimated percent change in lead at the point of use, comparing sample profiles collected at 1 mg PO_4 L^{-1} and again, approximately 1 year later, at 2 mg PO_4 L^{-1}. Model predictions generated using a flat prior (i.e., no prior knowledge of the effect of orthophosphate) are compared against those generated using a prior informed by the GAM. (*N* denotes the normal distribution.) **(b)** Lead at the point of use, paired by site and profile litre. Left-censored values (i.e., nondetects) are represented by the horizontal/vertical ticks and the grey-shaded region at the bottom left of the plot. The red diagonal line represents the estimated difference between lead concentrations at the two doses, and the red-shaded region represents a 95% credible interval on that estimate (generated using an informative $N(-0.8, 0.3)$ prior).

Geometric mean lead release at the high orthophosphate dose (2 mg PO_4 L^{-1}) was 60% of that at the low dose (1 mg PO_4 L^{-1}), with a 95% credible interval of 50–76% (Figure 2b). The choice of prior had little influence on the difference estimate: the corresponding estimate obtained by using an uninformative prior—assigning equal probability to all orthophosphate treatment effect sizes, whether physically plausible or not—was 63%, with a 95% credible interval of 52–84%.

These estimates are somewhat smaller than the one based on pipe rack data. Differences in the models are a factor, but differences in materials also matter. That is, pipe racks measure the response of lead pipe to orthophosphate treatment, which tends to be quite large at slightly basic pH and low dissolved inorganic carbon. Data from sentinel homes, though, also capture the effect of orthophosphate on lead release from other sources, which is much more ambiguous. Corrosion of lead solder, for instance, may be accelerated by orthophosphate.[52] To capture these effects, pipe racks could easily be modified to include copper and lead solder.

Quantifying the effect of an orthophosphate dose decrease

A little more than a year after the orthophosphate dose was increased in Zone 1, it was decreased from 2 to 1.5 mg PO_4 L^{-1} (Figure 3b). We used the sentinel pipe racks to determine the orthophosphate dose response in this zone. That is, we estimated the effect of an increase from 1 to 2 mg PO_4 L^{-1} and the effect of a subsequent decrease to 1.5 mg PO_4 L^{-1}. But since the final decrease occurred in the spring—as water temperatures were increasing rapidly (Figure 3e)—we estimated the seasonal variation in lead release and added it as a separate term in the model to control for temperature effects. Seasonality was more complex in Zone 2, perhaps due to the inverse seasonality in aluminum (especially before the change in coagulation pH[20]). And since the dose increases occurred in late November and July in Zones 1 and 2 respectively, controlling explicitly for seasonality in the full model—encompassing both zones—was less important.

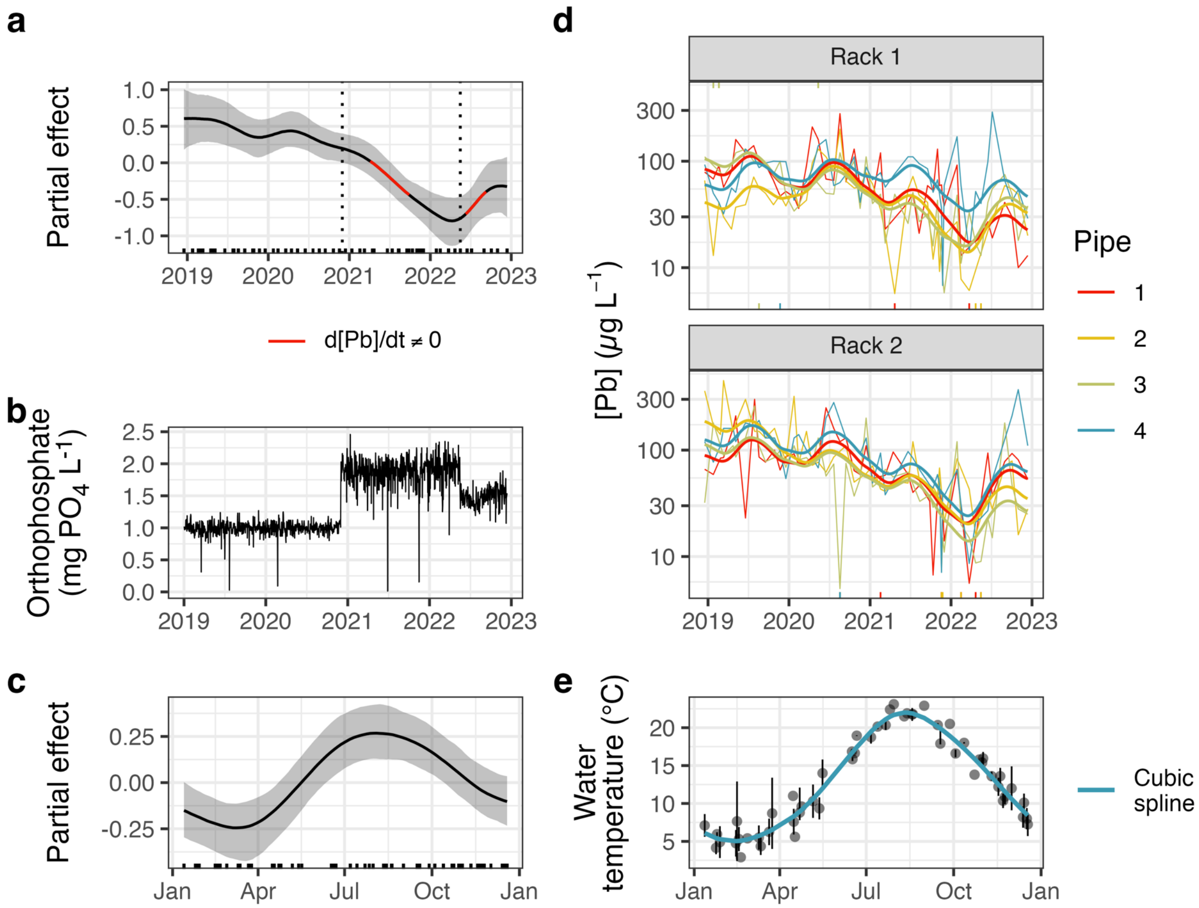

Figure 3. (a) The global multi-year trend in lead release; red highlighting indicates the portion of the trend where the 95% credible interval on its slope does not include zero. **(b)** Orthophosphate in Zone 1 treated water. **(c)** The seasonal smooth term in the GAM. In **(a)** and **(c)**, shaded grey regions span 95% credible intervals on the trends, and ticks on the x-axes represent sample collection dates. **(d)** Time series of total lead in effluent from lead pipes at the two locations in Zone 1. Fitted values from the hierarchical GAM are superimposed on the time series in bold. Ticks at the top and bottom of the panels represent values outside the plotting limits. **(e)** Water temperature in pipe rack effluent; points represent medians and error bars span the range of measurements, by date. A cyclic cubic spline[46] is superimposed in blue.

As in the full model, mean (log) lead concentrations were relatively constant at 1 mg PO_4 L^{-1}: at this dose, a 95% credible interval on the slope of the global multi-year trend always included 0 μg Pb L^{-1} d^{-1} (Figure 3a). An increase to 2 mg PO_4 L^{-1} was followed here as well by a decreasing trend in lead concentrations.

Even after accounting for the seasonal variation in lead release, though, a decrease in the orthophosphate dose to 1.5 mg PO_4 L^{-1} was followed by an increase in lead release

(Figure 3a) and a 95% credible interval on the slope of the global trend that did not include zero. The intermediate dose, then, appears to have yielded lead concentrations between those resulting from the 1 and 2 mg PO_4 L^{-1} doses. Six months after the orthophosphate dose reduction, the increase in geometric mean lead release was estimated at 55%, with a 95% credible interval of 5–143%.

This result has implications for passivation-maintenance orthophosphate dosing strategies—that is, initiating treatment at a high orthophosphate dose to promote lead phosphate scale formation and then decreasing the dose once scale evolution has slowed.[53] Although lead solubility is predicted to increase with a decrease in orthophosphate, the effect on particulate lead is unclear: an established lead-phosphate scale, for instance, may be no less durable after a decrease in the orthophosphate dose. But while passivation/maintenance dosing has the potential to conserve phosphorus, it should be evaluated carefully to avoid unwanted increases in lead release at the maintenance dose or excess particulate lead at an unnecessarily high passivation dose.[16,54] Here, the dose response of lead release to orthophosphate was qualitatively similar to that predicted by solubility: lead release decreased when orthophosphate was increased and increased when orthophosphate was decreased.

Conclusion

Point-of-use sampling is necessary to accurately quantify lead release into drinking water. But lead service line replacement, incomplete participation by residents in sampling programs, and changes to premises plumbing make it difficult to monitor the effectiveness of corrosion control over time this way. And while no simple apparatus can reliable quantify human exposure to lead, sentinel pipe racks offer an alternative to point-of-use sampling for non-regulatory monitoring. Especially when installed at multiple locations across a water distribution network, sentinel pipe racks can be used to understand how both anticipated and unexpected changes in water quality impact lead concentrations. We used them here to estimate the effect on lead release of changes in orthophosphate dose and coagulation process. By partitioning the variation in lead concentrations hierarchically—estimating global and location-level trends—we were better able to control for seasonality or other potential confounders before quantifying the effects of interest.

Acknowledgements

This work was supported by Mitacs, through the Mitacs Accelerate Program (Reference # IT23352), and NSERC, through an Industrial Research Chair program (Grant # IRCPJ: 349838-16). We acknowledge Halifax Water's water quality department for managing the pipe rack and residential sampling programs.

Supporting information

Graphical and tabular summaries of water quality, figures summarizing smooth terms not appearing in the body of the paper, instructions provided to volunteer residents, and a photo of a prototype pipe rack.

References

(1) Schock, M. R. Understanding Corrosion Control Strategies for Lead. *Journal - American Water Works Association* **1989**, *81* (7), 88–100. https://doi.org/10.1002/j.1551-8833.1989.tb03244.x.

(2) Dodrill, D. M.; Edwards, M. Corrosion Control on the Basis of Utility Experience. *Journal - American Water Works Association* **1995**, *87* (7), 74–85. https://doi.org/10.1002/j.1551-8833.1995.tb06395.x.

(3) Bae, Y.; Pasteris, J. D.; Giammar, D. E. Impact of Orthophosphate on Lead Release from Pipe Scale in High pH, Low Alkalinity Water. *Water Research* **2020**, *177*, 115764. https://doi.org/10.1016/j.watres.2020.115764.

(4) Doré, E.; Deshommes, E.; Laroche, L.; Nour, S.; Prévost, M. Study of the Long-Term Impacts of Treatments on Lead Release from Full and Partially Replaced Harvested Lead Service Lines. *Water Research* **2019**, *149*, 566–577. https://doi.org/10.1016/j.watres.2018.11.037.

(5) Lytle, D. A.; Schock, M. R.; Formal, C.; Bennett-Stamper, C.; Harmon, S.; Nadagouda, M. N.; Williams, D.; DeSantis, M. K.; Tully, J.; Pham, M. Lead Particle Size Fractionation and Identification in Newark, New Jersey's Drinking Water. *Environmental Science & Technology* **2020**, *54* (21), 13672–13679. https://doi.org/10.1021/acs.est.0c03797.

(6) Bae, Y.; Pasteris, J. D.; Giammar, D. E. The Ability of Phosphate To Prevent Lead Release from Pipe Scale When Switching from Free Chlorine to Monochloramine. *Environmental Science & Technology* **2020**, *54* (2), 879–888. https://doi.org/10.1021/acs.est.9b06019.

(7) Aghasadeghi, K.; Peldszus, S.; Trueman, B. F.; Mishrra, A.; Cooke, M. G.; Slawson, R. M.; Giammar, D. E.; Gagnon, G. A.; Huck, P. M. Pilot-Scale Comparison of Sodium Silicates, Orthophosphate and pH Adjustment to Reduce Lead Release from Lead Service Lines. *Water Research* **2021**, *195*, 116955. https://doi.org/10.1016/j.watres.2021.116955.

(8) Noel, J. D.; Wang, Y.; Giammar, D. E. Effect of Water Chemistry on the Dissolution Rate of the Lead Corrosion Product Hydrocerussite. *Water Research* **2014**, *54*, 237–246. https://doi.org/10.1016/j.watres.2014.02.004.

(9) Li, B.; Trueman, B. F.; Locsin, J. M.; Gao, Y.; Rahman, M. S.; Park, Y.; Gagnon, G. A. Impact of Sodium Silicate on Lead Release from Lead(II) Carbonate. *Environmental Science: Water Research & Technology* **2021**, *7* (3), 599–609. https://doi.org/10.1039/D0EW00886A.

(10) Wasserstrom, L. W.; Miller, S. A.; Triantafyllidou, S.; Desantis, M. K.; Schock, M. R. Scale Formation Under Blended Phosphate Treatment for a Utility With Lead Pipes. *Journal - American Water Works Association* **2017**, *109*, E464–E478. https://doi.org/10.5942/jawwa.2017.109.0121.

(11) Tully, J.; DeSantis, M. K.; Schock, M. R. Water Quality–Pipe Deposit Relationships in Midwestern Lead Pipes. *AWWA Water Science* **2019**, *1* (2), e1127. https://doi.org/10.1002/aws2.1127.

(12) Trueman, B. F.; Anaviapik-Soucie, T.; L'Hérault, V.; Gagnon, G. A. Characterizing Colloidal Metals in Drinking Water by Field Flow Fractionation. *Environmental Science: Water Research & Technology* **2019**, *5* (12), 2202–2209. https://doi.org/10.1039/C9EW00560A.

(13) Health Canada. *Guidance on sampling and mitigation measures for controlling corrosion - guidance document for public consultation*. https://www.canada.ca/en/health-canada/programs/consultation-draft-guidance-sampling-mitigation-measures-controlling-corrosion.html (accessed 2023-01-16).

(14) Devine, C.; Triantafyllidou, S. A Literature Review of Bench Top and Pilot Lead Corrosion Assessment Studies. *AWWA Water Science* **2023**, *5* (2), e1324. https://doi.org/10.1002/aws2.1324.

(15) Masters, S. V.; Poncelet-Johnson, N.; Walsh, R.; Seidel, C. J.; Corwin, C. J. Comparison of Coupon and Pipe Rack Studies for Selecting Corrosion Control Treatment. *AWWA Water Science* **2022**, *4* (4). https://doi.org/10.1002/aws2.1293.

(16) Trueman, B. F.; James, W.; Shu, T.; Doré, E.; Gagnon, G. A. Comparing Corrosion Control Treatments for Drinking Water Using a Robust Bayesian Generalized Additive Model. *ACS ES&T Engineering* **2022**, 15–25. https://doi.org/10.1021/acsestengg.2c00194.

(17) Krkošek, W.; Healey, M.; Sampson, C.; McKnight, A. Halifax Water's Lead Service Line Replacement Program Gets the Lead Out. *Journal AWWA* **2022**, *114* (2), 10–19. https://doi.org/10.1002/awwa.1862.

(18) Schock, M. R.; Wagner, I.; Oliphant, R. J. Corrosion and solubility of lead in drinking water. In *Internal corrosion of water distribution systems*; American Water Works Association Research Foundation: Denver, CO, 1996; pp 131–230.

(19) Trueman, B. F.; Krkošek, W. H.; Gagnon, G. A. Effects of Ortho- and Polyphosphates on Lead Speciation in Drinking Water. *Environmental Science: Water Research & Technology* **2018**, *4* (4), 505–512. https://doi.org/10.1039/C7EW00521K.

(20) Trueman, B. F.; Bleasdale-Pollowy, A.; Locsin, J. A.; Bennett, J. L.; Krkošek, W. H.; Gagnon, G. A. Seasonal Lead Release into Drinking Water and the Effect of Aluminum. *ACS ES&T Water* **2022**, 710–720. https://doi.org/10.1021/acsestwater.1c00320.

(21) Harmon, S. M.; Tully, J.; DeSantis, M. K.; Schock, M. R.; Triantafyllidou, S.; Lytle, D. A. A Holistic Approach to Lead Pipe Scale Analysis: Importance, Methodology, and Limitations. *AWWA Water Science* **2022**, *4* (2). https://doi.org/10.1002/aws2.1278.

(22) USEPA. *Method 6020B (SW-846): Inductively Coupled Plasma-Mass Spectrometry, Revision 2.*; 2014.

(23) 5310 Total Organic Carbon. In *Standard methods for the examination of water and wastewater*. https://doi.org/10.2105/SMWW.2882.104.

(24) 4500-Cl Chloride. In *Standard methods for the examination of water and wastewater*. https://doi.org/10.2105/SMWW.2882.079.

(25) ASTM International. *Standard test method for sulfate ion in water.* https://www.astm.org/d0516-16.html.

(26) 4500-P Phosphorus. In *Standard methods for the examination of water and wastewater*. https://doi.org/10.2105/SMWW.2882.093.

(27) USEPA. *Method 310.2: Alkalinity (Colorimetric, Automated, Methyl Orange) by Autoanalyzer*; 1974.

(28) R Core Team. *R: A language and environment for statistical computing*. https://www.R-project.org/.

(29) Allaire, J.; Xie, Y.; McPherson, J.; Luraschi, J.; Ushey, K.; Atkins, A.; Wickham, H.; Cheng, J.; Chang, W.; Iannone, R. *rmarkdown: Dynamic documents for R*. https://github.com/rstudio/rmarkdown.

(30) Wickham, H.; Averick, M.; Bryan, J.; Chang, W.; McGowan, L. D.; François, R.; Grolemund, G.; Hayes, A.; Henry, L.; Hester, J.; Kuhn, M.; Pedersen, T. L.; Miller, E.; Bache, S. M.; Müller, K.; Ooms, J.; Robinson, D.; Seidel, D. P.; Spinu, V.; Takahashi, K.; Vaughan, D.; Wilke, C.; Woo, K.; Yutani, H. Welcome to the tidyverse. *Journal of Open Source Software* **2019**, *4* (43), 1686. https://doi.org/10.21105/joss.01686.

(31) Wickham, H.; Bryan, J. *readxl: Read excel files*. https://CRAN.R-project.org/package=readxl.

(32) Firke, S. *janitor: Simple tools for examining and cleaning dirty data*. https://CRAN.R-project.org/package=janitor.

(33) Fischetti, T. *assertr: Assertive programming for r analysis pipelines*. https://CRAN.R-project.org/package=assertr.

(34) Bürkner, P.-C. brms: An R Package for Bayesian Multilevel Models Using Stan. *Journal of Statistical Software* **2017**, *80* (1), 1–28. https://doi.org/10.18637/jss.v080.i01.

(35) Kay, M. *ggdist: Visualizations of distributions and uncertainty*. https://doi.org/10.5281/zenodo.3879620.

(36) Hester, J.; Bryan, J. *glue: Interpreted string literals*. https://CRAN.R-project.org/package=glue.

(37) Bürkner, P.-C.; Gabry, J.; Kay, M.; Vehtari, A. *posterior: Tools for working with posterior distributions*. https://mc-stan.org/posterior/.

(38) Wickham, H. testthat: Get Started with Testing. *The R Journal* **2011**, *3*, 5–10.

(39) Gabry, J.; Mahr, T. *bayesplot: Plotting for bayesian models*. https://mc-stan.org/bayesplot/.

(40) Pedersen, T. L. *patchwork: The composer of plots*. https://CRAN.R-project.org/package=patchwork.

(41) Wilke, C. O.; Wiernik, B. M. *ggtext: Improved text rendering support for 'ggplot2'*. https://CRAN.R-project.org/package=ggtext.

(42) Wickham, H.; Hester, J.; Chang, W.; Bryan, J. *devtools: Tools to make developing r packages easier*. https://CRAN.R-project.org/package=devtools.

(43) Wood, S. N. *Generalized Additive Models: An Introduction with r*, 2nd ed.; Chapman; Hall/CRC, 2017.

(44) Trueman, B. *Source code for "Sentinel pipe racks quantify orthophosphate's effect on lead release into drinking water"*. https://github.com/bentrueman/cct-monitoring.

(45) Trueman, B. *bgamcar1: Fit bayesian GAMs with CAR(1) errors to censored data*. https://github.com/bentrueman/bgamcar1.

(46) Pedersen, E. J.; Miller, D. L.; Simpson, G. L.; Ross, N. Hierarchical Generalized Additive Models in Ecology: An Introduction with mgcv. *PeerJ* **2019**, *7*, e6876. https://doi.org/10.7717/peerj.6876.

(47) Simpson, G. L. Modelling Palaeoecological Time Series Using Generalised Additive Models. *Frontiers in Ecology and Evolution* **2018**, *6*, 149. https://doi.org/10.3389/fevo.2018.00149.

(48) McElreath, R. *Statistical Rethinking: A Bayesian Course with Examples in R and Stan*; Chapman & Hall/CRC texts in statistical science series; CRC Press/Taylor & Francis Group: Boca Raton, 2016.

(49) Gelman, A. Bayes, Jeffreys, Prior Distributions and the Philosophy of Statistics. *Statistical Science* **2009**, *24* (2). https://doi.org/10.1214/09-STS284D.

(50) Edzwald, J. K. Aluminum in Drinking Water: Occurrence, Effects, and Control. *Journal AWWA* **2020**, *112* (5), 34–41. https://doi.org/10.1002/awwa.1499.

(51) Korshin, G. V.; Ferguson, J. F.; Lancaster, A. N.; Wu, H. *Corrosion and Metal Release for Lead-Containing Materials: Influence of NOM*; AWWA Research Foundation; American Water Works Association: Denver, 1999.

(52) Nguyen, C. K.; Clark, B. N.; Stone, K. R.; Edwards, M. A. Acceleration of Galvanic Lead Solder Corrosion Due to Phosphate. *Corrosion Science* **2011**, *53* (4), 1515–1521. https://doi.org/10.1016/j.corsci.2011.01.016.

(53) Schock, M. R.; Clement, J. Lead and Copper Control with Non-Zinc Orthophosphate. *Journal - New England Water Works Association* **1998**, *112*, 20–20.

(54) Zhao, J.; Giammar, D. E.; Pasteris, J. D.; Dai, C.; Bae, Y.; Hu, Y. Formation and Aggregation of Lead Phosphate Particles: Implications for Lead Immobilization in Water Supply Systems. *Environmental Science & Technology* **2018**, *52* (21), 12612–12623. https://doi.org/10.1021/acs.est.8b02788.

Supplementary information for: Sentinel pipe racks quantify orthophosphate's effect on lead release into drinking water

Benjamin F. Trueman[§,*], Wendy H. Krkošek[†], and Graham A. Gagnon[§]

[§]Centre for Water Resources Studies, Department of Civil & Resource Engineering, Dalhousie University, 1360 Barrington St., Halifax, Nova Scotia, Canada B3H 4R2

[†]Halifax Water, 450 Cowie Hill Rd., Halifax, Nova Scotia, Canada, B3P 2V3

*Corresponding author
E-mail: benjamin.trueman@dal.ca
Tel:902.494.6070
Fax: 902.494.3105

This document has 5 pages, 5 figures, and 1 table.

Table S1. Summary of water quality in pipe rack effluent, by zone.

Parameter	Unit	Zone	Median	Lower quartile	Upper quartile
Conductivity	mS	1	142.0	133.0	153.0
		2	87.0	82.0	93.0
Dissolved Chloride	mg L^{-1}	1	8.4	7.8	9.2
		2	8.6	7.9	9.6
Dissolved Inorganic Carbon	mg C L^{-1}	1	4.6	4.3	5.0
		2	3.7	3.3	4.3
Dissolved Sulfate	mg SO_4 L^{-1}	1	32.0	29.0	36.0
		2	9.6	8.7	11.0
Dissolved Oxygen	mg L^{-1}	1	10.0	9.1	11.8
		2	10.2	9.6	12.0
Free Chlorine		1	0.5	0.1	0.7
		2	0.7	0.6	0.8
Total Organic Carbon	mg C L^{-1}	1	1.8	1.7	2.0
		2	1.8	1.8	2.1
ORP	mV	1	516.0	435.5	624.0
		2	422.0	375.0	527.0
Orthophosphate (phase 1)	mg P L^{-1}	1	0.2	0.2	0.3
		2	0.3	0.2	0.3
Orthophosphate (phase 2)		1	0.5	0.5	0.6
		2	0.6	0.5	0.7
pH		1	7.3	7.1	7.4

Parameter	Unit	Zone	Median	Lower quartile	Upper quartile
		2	7.4	7.3	7.6
Temperature	C	1	12.5	7.1	17.8
		2	10.5	6.5	17.4
Total Alkalinity	mg $CaCO_3$ L^{-1}	1	23.0	21.0	25.0
		2	19.0	16.0	21.0
Total Aluminum	μg L^{-1}	1	11.0	9.2	13.0
		2	38.0	23.0	70.8
Total Iron		1	25.0	25.0	25.0
		2	25.0	25.0	25.0
Total Lead		1	59.0	36.0	95.5
		2	85.0	26.8	190.0
Total Manganese		1	1.0	1.0	2.5
		2	3.2	2.3	4.9
Total Zinc		1	180.0	150.0	220.0
		2	190.0	160.0	210.0
Turbidity	NTU	1	0.1	0.1	0.2
		2	0.1	0.1	0.2

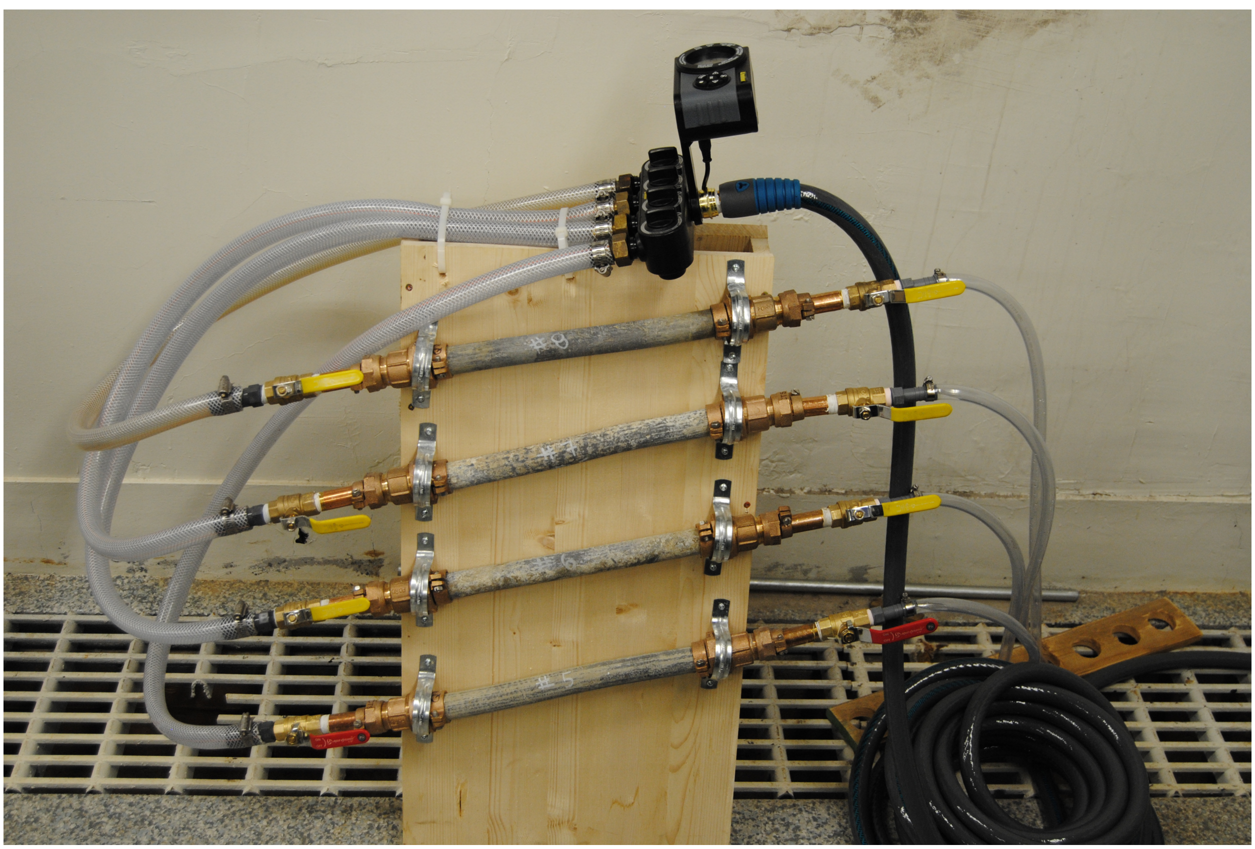

Figure S1. An example of the pipe racks installed in Zones 1 and 2.

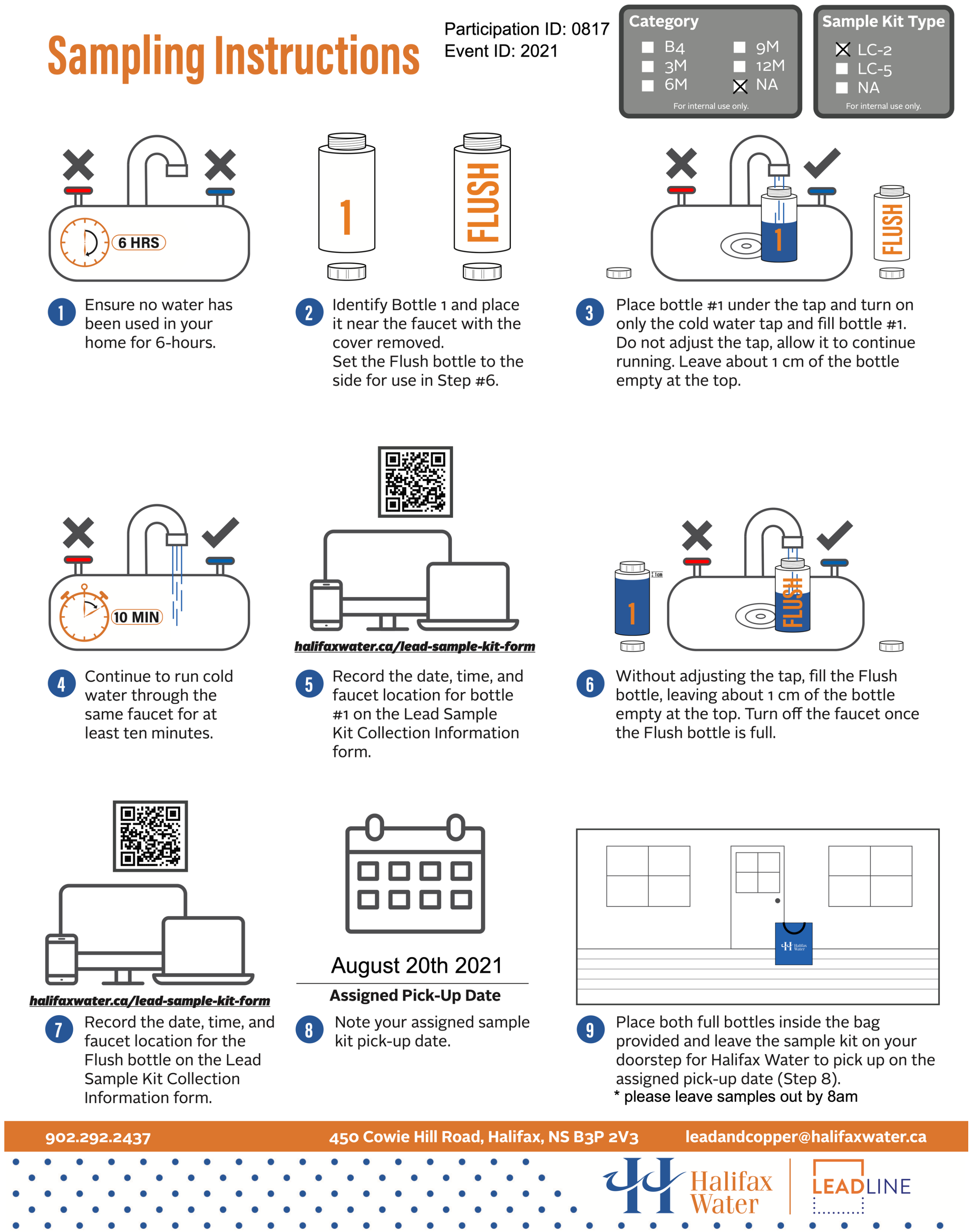

Figure S2. An example instruction sheet distributed to volunteer residents collecting point-of-use samples from sentinel homes.

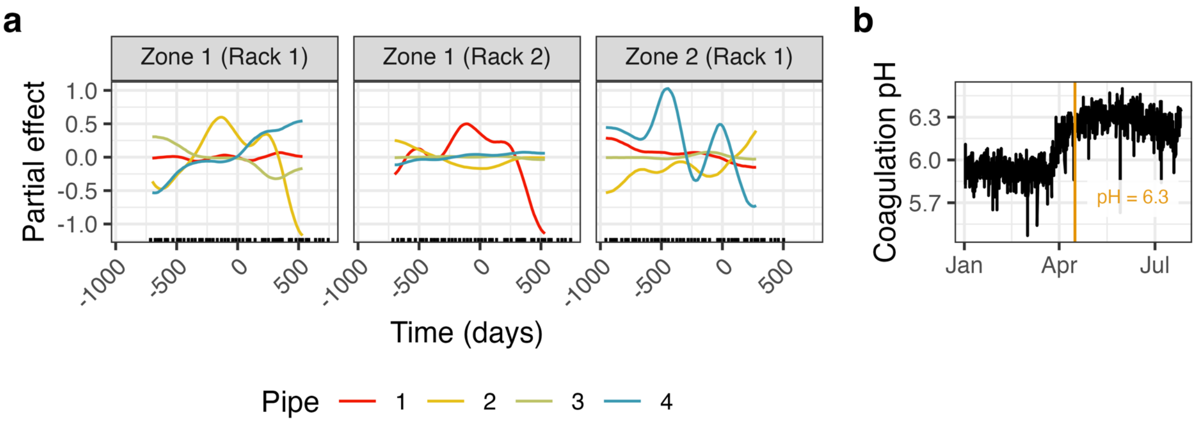

Figure S3. (a) In the full (Zones 1 and 2) model, local multi-year smooths capturing the deviations of each series from the global and location-specific smooths. **(b)** Coagulation pH at the treatment plant supplying Zone 2.

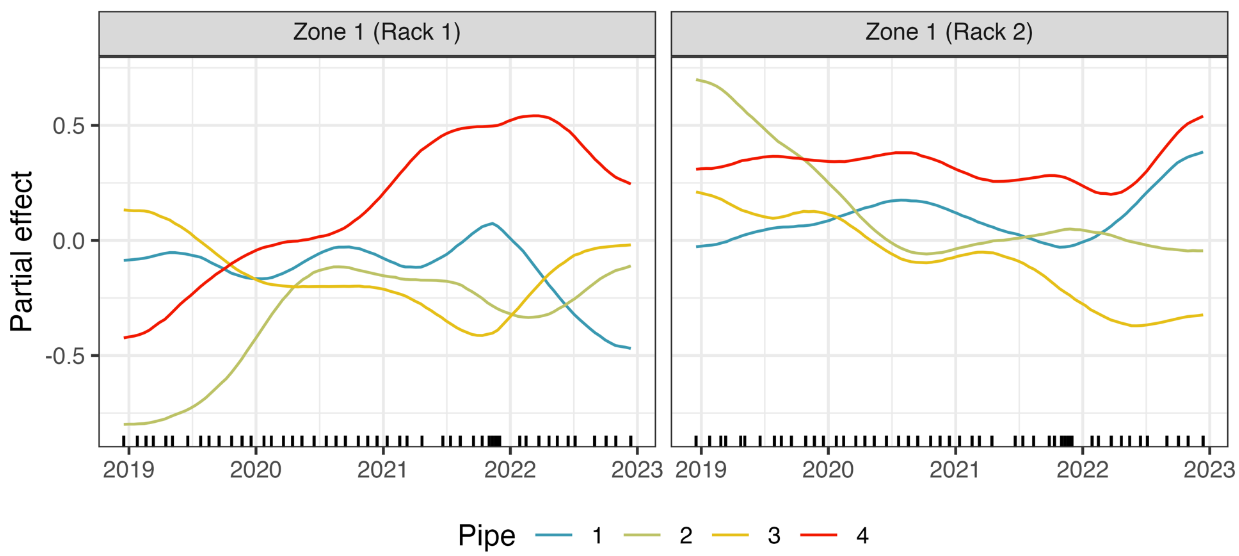

Figure S4. In the Zone 1 model, local multi-year smooths capturing the deviations of each series from the global and seasonal smooths.

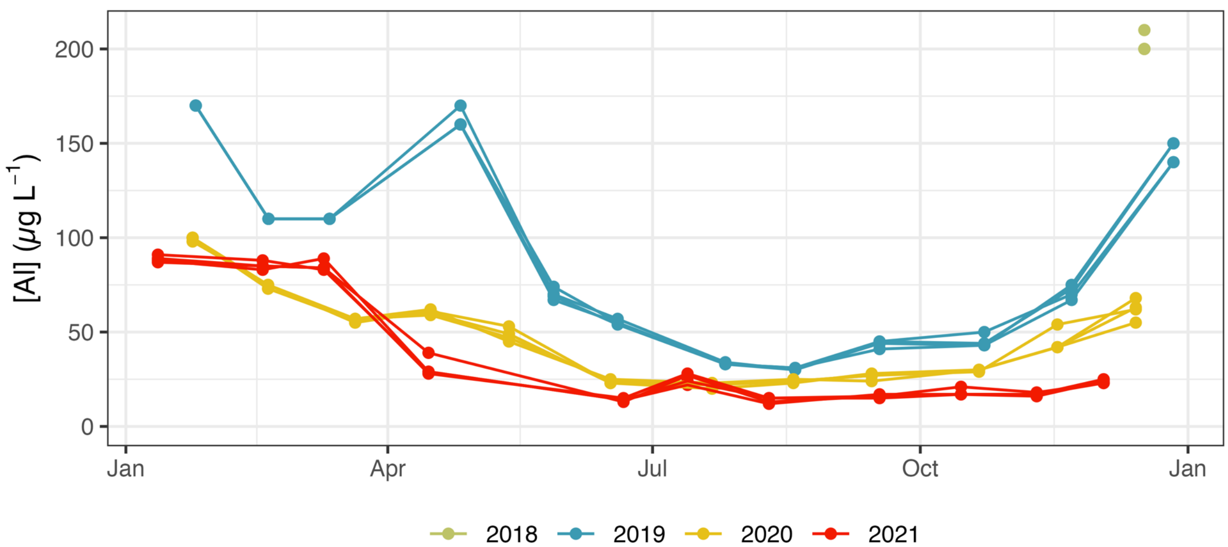

Figure S5. Total aluminum in pipe rack effluent.